# DISCUSSION OF TWO-PHOTON LASER-EXCITED FLUORESCENCE AS A METHOD FOR QUANTITATIVE DETECTION OF OXYGEN ATOMS IN FLAMES

U. MEIER, J. BITTNER, K. KOHSE-HÖINGHAUS AND TH. JUST

*DFVLR-Institut für Physikalische Chemie der Verbrennung; Pfaffenwaldring 38-40, 7000 Stuttgart 80, W. Germany*

Spatially resolved measurements of absolute oxygen atom concentrations in low-pressure $H_2/O_2/Ar$-, $CH_4/O_2$- and $C_2H_2/O_2$ flames are performed by two-photon laser excited fluorescence. The measured signals are converted into O atom number densities using a calibration technique, based on the comparison of fluorescence signals in a flame with those in a discharge flow reactor. This procedure requires consideration of quenching processes; furthermore, the influence of photoionization and potential photodissociation of flame gases must be considered. The sensitivity of the derived concentrations to experimental parameters and atomic quantities is discussed.

## Introduction

The general goal of our fluorescence experiments in flames is to compile a consistent set of experimental data on concentrations of radical species under a variety of flame conditions. We want to apply consequently nonperturbative methods for the measurements of radical concentrations like O, H, N, OH, CH, NH etc. in selected flames in order to avoid the wellknown difficult problems of flame distortion by probes. The thus obtained database is intended to serve for comparison with the results of chemical-kinetic models of the corresponding flames, in order to test again and possibly improve further existing numeric models. For this compilation, low-pressure laminar premixed flames of selected fuels, namely $H_2$, $CH_4$ and $C_2H_2$ are investigated. The kinetic mechanism for the oxidation of these fuels may then be included as a subsystem in the reaction system of more complex hydrocarbons.

Measurements of temperature and OH concentration profiles in $H_2$, $CH_4$, and $C_2H_2$ flames have been reported,[1] as well as CH concentrations in $C_2H_2/O_2$ flames.[2] Recently, we developed a method for quantitative H atom detection in flames using two-photon laser-excited fluorescence.[3] Our method will now be applied to O atoms.

Oxygen atoms have been detected in flames by different optical methods: spontaneous Raman scattering[4] and CARS,[5] as well as fluorescence[6,7,8] or optogalvanic[9,10] detection after two-photon excitation. For the determination of absolute concentration in flames, only one indirect method was reported.[10]

Our approach to derive quantitative O atom concentrations from two-photon excited fluorescence signals is the same as used for H atoms earlier.[3] Since flames are opaque for VUV radiation necessary for single photon excitation of oxygen atoms, two-photon excitation at correspondingly longer wavelengths is a suitable alternative optical detection method. In such an experiment, however, fluorescence signals depend strongly on the laser power density, which can be determined only with limited accuracy, since the laser beam has to be focussed to obtain fluorescence signals with sufficient signal-to-noise ratio. In addition, the excitation rate is determined by the two-photon transition probability, which is not known with sufficient precision in many cases. Due to these complications, a direct measurement of atom concentrations from known experimental parameters and atomic transition probabilities is not trivial. Therefore, we apply a calibration technique based on the comparison of fluorescence signals in the flame with those from known atom concentrations, generated in a discharge flow reactor. The basic idea of this procedure is to diminish, if not to cancel, the influence of experimental parameters and atomic quantities when identical excitation/detection conditions are maintained. However, due to different pressures and gas compositions in flame and discharge flow reactor, respectively, several effects have to be considered which could lead to erroneous atom concentrations if neglected. These effects are: quenching, photoionization, and photodissociation. The latter has already been shown to be a serious source of errors in the quantitative detection of atoms under unfavourable conditions.[6,7,8,11] In particular this is true for flames at atmospheric pressure and at high temperatures. In the following, we

shall discuss the calibration technique and show how the influence of quenching can be taken into account. The effect of such quantities as two-photon transition probabilities, laser power density, photoionization and -dissociation cross sections, which are known only with limited accuracy, on the determination of O atom concentrations is investigated. Finally, we present measurements of O atom concentrations in selected $H_2/O_2/Ar$ flames where temperature-, OH-, and H concentration profiles have been measured earlier.

## Experiment

The experimental arrangement was basically identical to that used earlier for H atom experiments.[3,12] Oxygen atoms in the discharge flow reactor were produced by the reaction $N + NO \rightarrow O + N_2$. The nitrogen atoms were generated in a microwave discharge in $N_2$, diluted in helium. The flow reactor was operated at pressures between 2.5 and 10 mbar (1.9 to 7.5 Torr) and total flow rates of about 2 slm. The initial O atom concentrations ranged from $5 \cdot 10^{13}$ to $5 \cdot 10^{14}$ cm$^{-3}$; they were determined from NO mole fractions and pressure under conditions where total conversion of NO into O was assured.

Oxygen atoms were excited at the downstream end of the flow tube using 226 nm radiation from a frequency doubled, Nd:YAG pumped dye laser running with a mixture of Rhodamine 6G and Rhodamine B; its output was mixed with the residual infrared radiation of the YAG laser. Pulse energies of up to 4 mJ at 226 nm with an average bandwidth of about 2 cm$^{-1}$ were thus obtained. The radiation was focussed by a $f = 50$ cm lens into the flow reactor. To avoid strong saturation of the excited $2p^3P - 3p^3P$ two-photon transition or ionization of the $3p^3P$ state, the laser was attenuated to pulse energies less than 1 mJ, and the lens was placed to the flow tube at a distance closer than the focal length. Under these conditions, the focal beam diameter at the detection volume was about 400 μm; this was measured by scanning a 100 μm diaphragm across the beam profile. The peak power was determined with a calibrated fast vacuum photodiode. The resulting power density was usually 100 to 200 MW/cm$^2$. Fluorescence signals were passed through an interference filter at 845 nm with a FWHM of 12 nm and imaged by a $f/4.5$ lens onto the cathode of a R636 multiplier (Hamamatsu). From the observed solid angle and the burner diameter of 42 mm., it follows that fluorescence cutoff by the burner occurs at heights less than 2.3 mm; this effect was taken into account by geometrical considerations. Signals were averaged over typically 100 laser pulses; the peak intensities were evaluated. Under these conditions, the signal-to-noise

ratio was always better than 10:1, even at low O atom concentrations in the calibration runs or in experiments with low laser intensities for power dependence measurements.

## Fundamental Relations

We shall discuss the calibration technique in more detail by means of the differential equations governing the populations of the atomic states. The states and processes involved in the two-photon excitation process of O atoms are shown in Fig. 1. Using the notation of Fig. 1 for the states, the populations $N_i$ are given approximately by the following expressions:

$$\frac{dN_1}{dt} = -N_1 \cdot W_{12} + N_2 \cdot (Q_{21} + W_{21})$$
$$+ N_3 \cdot (A_{31} + Q_{31}) + N_0 \cdot W_{diss} \quad (1a)$$

$$\frac{dN_2}{dt} = N_1 \cdot W_{12}$$
$$- N_2 \cdot (Q_{23} + Q_{21} + W_{21} + P_{2i} + A_{23}) \quad (1b)$$

$$\frac{dN_3}{dt} = N_2 \cdot (Q_{23} + A_{23})$$
$$- N_3 \cdot (A_{31} + Q_{31} + P_{3i}) \quad (1c)$$

$N_i \cdot A_{ij}$ and $N_i \cdot Q_{ij}$ are the rates for spontaneous emission and quenching from state $i$ to state $j$; $Q_{ij}$ is given by the relation

$$Q_{ij} = \sum_k k_{ij}^k(T) \cdot N_k, \quad (2)$$

where $k_{ij}^k(T)$ is the temperature-dependent rate coefficient for quenching from state $i$ to state $j$ by the collision partner $k$; the summation has to be performed over all collision partners present in the flame. $W_{12}$ is the two-photon transition rate coefficient, given by[14] $W_{12} = \alpha_{12} \cdot I_L^2/h \cdot \nu_L$; $\alpha_{12}$ is the two-photon absorption cross section, $I_L$ the laser power density, and $h$ is Planck's constant. Correspondingly, $W_{21}$ describes stimulated two-photon emission from state 2 to state 1. $P_{ki}$ are the rate coefficients for photoionization of state $k$ ($k = 2,3$), given by $P_{ki} = \sigma_{ki} \cdot I_L/h \cdot \nu_L$, where $\sigma_{ki}$ is the photoionization cross section for state $k$. $N_0 \cdot W_{diss}$ is the rate for population of the O atom ground state by photodissociation of a potential precursor molecule with concentration $N_0$; $W_{diss} = \sigma_{diss} \cdot I_L/h \cdot \nu_L$, where $\sigma_{diss}$ is the photodissociation cross section for the precursor molecule.

This system of differential equations was solved numerically for different values of the parameters
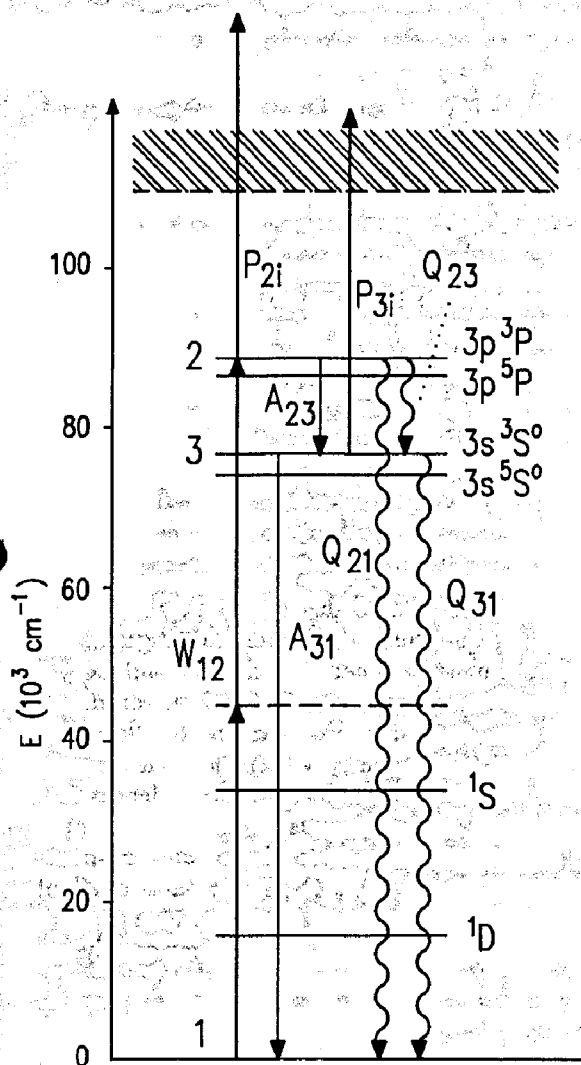
FIG. 1. Energy levels and processes involved in two-photon excitation/fluorescence detection of oxygen atoms

discussed above. These calculations served two purposes.

First, the larger influence of quenching in flames compared to flow reactor conditions can be taken into account by solving the equations for values of the quenching rates $Q_{ij}$ corresponding to reactor and flame conditions. The calculated ratio of the maximum populations of state 2 for each case, which are proportional to the peak fluorescence intensities, defines a "calibration factor" $C_Q$ which is a direct measure for the loss of fluorescence intensity due to quenching under flame conditions: $C_Q = N_{2,max}(Q_{reactor})/N_{2,max}(Q_{flame})$. Later, we shall describe how the values for $C_Q$ are obtained.

The second purpose of the numerical solutions of the differential equation is to obtain information on the sensitivity of the calibration technique to uncertainties of quantities like $\sigma_{12}$, $\sigma_{2i}$, $\sigma_{diss}$ or $I_L$. It will be shown how saturation due to high power

densities, strong photoionization or additional atom production by photodissociation affect atom concentration measurements.

Our experiments allow no determination of the branching ratios between the quenching rates to different final states; instead, only total removal rates $Q_2$ from state 2 could be measured. Investigation of the differential equations showed that the quantity of interest, namely the population of state 2, is not significantly altered if either a "cascading" process or direct quenching from state 2 to state 1 is assumed. Ionization of state 3 has no noticeable effect on the population of state 2 and has therefore been disregarded in the calculations. Furthermore, fine structure splitting is also neglected. Since the splitting of the three fine structure levels of the $2p^3P$ ground state is large compared to the laser bandwidth, excitation occurs only from one component. For reasons of intensity, we generally used excitation from $J'' = 2$. This state has the additional advantage of a relatively small temperature dependence of the relative population; the Boltzmann fraction changed by less than 7% with temperature for all flames. According to two-photon transition probabilities, all three fine structure levels of the $3p^3P$ state are populated,[13] since the laser bandwidth is too large to resolve the splitting of the fine structure components in the excited state. Therefore, $Q_2$, $W_{2i}$ and $A_{23}$ must be considered as averaged quantities.

## Results and Discussion

*Calibration:*

In a typical experiment, first a calibration measurement was performed in the discharge flow reactor, which yielded the sensitivity for the detection of oxygen atoms at the particular experimental conditions given. Then the reactor was replaced by the low-pressure burner, and O atom fluorescence signals in different flames were recorded, while all other parameters like laser beam profile, laser power, and detection optics, remained the same. Under these conditions, the oxygen atom concentration $[O]_B$ at a given position in a flame is given by

$$[O]_B = \frac{I_{fl,B}}{I_{fl,R}} \cdot [O]_R \cdot \frac{B(T_R)}{B(T_B)} \cdot C_Q \qquad (3)$$

Here, $I_{flB}$ and $I_{flR}$ are the measured fluorescence intensities in the burner and the reactor, respectively; $[O]_R$ is the atom concentration in the flow reactor. $B(T_R)$ and $B(T_B)$ are the relative populations in the $J'' = 2$ level at reactor and flame temperature, respectively. $C_Q$ is the position-dependent calibration factor for quenching and will be discussed.

If relative fluorescence intensities in the flow reactor are plotted as a function of NO concentration, a linear correlation is obtained for up to 90% conversion of the N atoms. At still higher NO number densities, the curve levels out due to total consumption of the initially generated N atoms. The slope of the linear part of the curve yields the O atom detection sensitivity. In our case, the slope had a standard deviation of 2%; if geometries and laser beam profiles were not too drastically altered, the slope could be reproduced from day to day within $\approx 5\%$.

*Quenching:*

For the determination of the calibration factor $C_Q$, the quenching rate $Q_2$ must be known as a function of temperature and position in the flame.

*Measurement of Quenching Rates in Flames:*

In a first approach to obtain values for $Q_2$, we measured individual rate coefficients for quenching of O atoms in the discharge flow reactor for all collision partners that are relevant in the flame.[3] These rate coefficients showed only weak temperature dependence between room temperature and about 700 K, so we used the measured room temperature values to calculate $Q_2$ for flame conditions according to Eq. (2). The required concentrations of the stable components in the flames were taken from model calculations using the code of Warnatz.[16]

In a second approach to obtain quenching rates under flame conditions, we tried to derive them from temporal fluorescence decays directly. This was possible since the quenching rate coefficients for oxygen atoms are sufficiently low, so that at the pressures of our flames the decay rates were only moderately fast. Nevertheless, the time response of the photomultiplier had to be considered. This was done by solving the system of differential equations for different values of $Q_2$ and convoluting the resulting time evolutions of $N_2$ with the photomultiplier response function. The resulting "synthetic" decay curves had now to be compared with the measured ones. As a criterion for the quality of the agreement between measured and simulated decay curves, we choose the integral under the curves, after normalizing them to a common maximum value.

Figure 2 shows an example for this procedure. The dashed line represents a measured fluorescence time profile in a lean ($\Phi = 0.6$) $CH_4/O_2$ flame, $p = 40$ mbar (flame 4), at 1 mm height above the burner. The continuous lines are synthetic profiles for values for $Q_2$ of 1, 2 and $3 \cdot 10^8$ s$^{-1}$. Very good agreement is found for $2 \cdot 10^8$ s$^{-1}$; the integrals of the measured and synthetic time decay differed by 0.8% in this case. Random tests like this have been performed for several other flames with

different decay rates. The method is applicable in our case for quenching rates up to about $4 \cdot 10^8$ s$^{-1}$; this limit is set by the response time of the photomultiplier used.

In Table I, quenching rates at selected heights above the burner measured in this way are assembled for all flames that have been investigated in this study. For comparison, we included values for the quenching rates that result from gas composition and room temperature quenching rate coefficients; it can be seen that these values are generally considerably higher than the directly measured ones. This indicates that the quenching rate and hence the calibration factor $C_Q$ cannot be determined reliably from gas composition and room temperature quenching rate coefficients. The ratios of the quenching rates between different flames reflect coarsely the respective $H_2O$ concentrations, which is plausible since measurements at room temperature showed that water is by far the most efficient quencher of all gases investigated. However, it must be noted that also CO and $CO_2$, and in the reaction zone, the fuel and $O_2$ contribute to the quenching rate. Furthermore the flames have different temperatures, which affect the quenching rate via possible temperature dependences of the individual rate coefficients.

The most instructive flame with respect to quenching is no. 10, a $H_2/O_2/Ar$ flame at 27 mbar and equivalence ratio of $\Phi = 0.6$. Due to the low pressure, the quenching rate is comparatively small, so that it can be determined with high accuracy and is furthermore practically not influenced by the response time of the photomultiplier. The quenching rate can be determined directly by fitting an exponential decay to the measured curve, which provides a test for the method of determining quenching rates by integration described above. The burnt gas of this flame consists of argon (66%), $H_2O$ (18.3%)
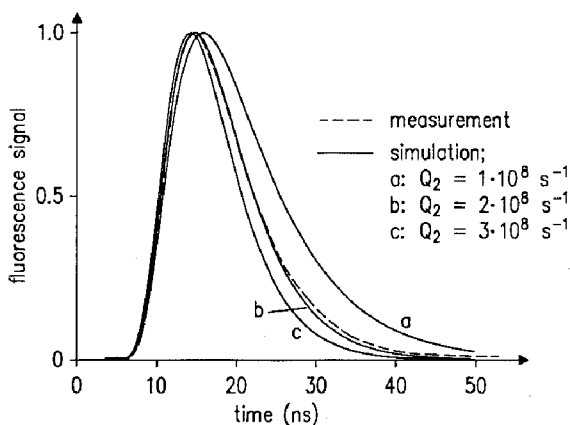


FIG. 2. Measured (– – –) and simulated (——) time decays of O atom fluorescence signals for different quenching rates; fluorescence signals in arbitrary units

## TABLE I

Quenching rates for oxygen atoms in low pressure flames. Pressures were 95 mbar (72 Torr) for flames 1–3, 40 mbar (30 Torr) for flames 4–9 and 27 mbar (20 Torr) for flame 10. a: directly determined from time decays of fluorescence signals, b: calculated from room temperature quenching rate coefficients and mole fractions of stable compounds

| | | | Quenching Rate ($10^8$ s$^{-1}$) | | | | | | | | | |
|---|---|---|---|---|---|---|---|---|---|---|---|---|
| | | | Height above burner (mm) | | | | | | | | | |
| Flame no. | Type | Mix. Frac. | 1 | | 2 | | 5 | | 10 | | 20 | |
| | | | a | b | a | b | a | b | a | b | a | b |
| 1 | $H_2/O_2/Ar$ | 0.6 | 2.50 | 5.20 | 2.30 | 5.10 | 2.00 | 5.60 | 1.90 | 5.50 | 1.80 | 5.90 |
| 2 | $H_2/O_2/Ar$ | 1.0 | 2.75 | 8.00 | 2.25 | 8.50 | 1.95 | 8.90 | 1.90 | 8.30 | — | — |
| 3 | $H_2/O_2/Ar$ | 1.4 | 3.25 | 8.50 | 3.05 | 9.00 | 2.50 | 10.0 | 2.50 | 10.0 | — | — |
| 4 | $CH_4/O_2$ | 0.6 | 2.00 | 3.30 | 1.90 | 3.10 | 1.90 | 3.00 | 1.85 | 3.00 | 1.95 | 3.30 |
| 5 | $CH_4/O_2$ | 1.2 | 1.90 | 3.50 | 1.60 | 3.80 | 1.55 | 4.10 | 1.55 | 4.10 | — | — |
| 6 | $CH_4/O_2$ | 1.6 | 2.00 | 3.30 | 1.85 | 3.25 | 1.40 | 3.20 | 1.50 | 3.20 | 1.65 | 3.20 |
| 7 | $C_2H_2/O_2$ | 0.6 | 1.70 | 2.40 | 1.75 | 1.90 | 1.60 | 2.00 | 1.60 | 2.00 | 1.60 | 2.00 |
| 8 | $C_2H_2/O_2$ | 1.2 | 1.45 | 2.70 | 1.40 | 2.70 | 1.25 | 2.60 | 1.30 | 2.60 | 1.40 | 2.60 |
| 9 | $C_2H_2/O_2$ | 1.6 | 1.00 | 2.90 | 1.20 | 2.60 | 1.10 | 2.40 | 1.18 | 2.40 | 1.35 | 2.40 |

| | | | 20 | | 30 | | 40 | |
|---|---|---|---|---|---|---|---|---|
| | | | a | b | a | b | a | b |
| 10 | $H_2/O_2/Ar$ | 0.6 | 1.50 | — | 0.75 | — | 0.60 | — |

and only a few percent of $H_2$ and $O_2$, its temperature is 1350 K. Here, water contributes largest to the quenching rate. The room temperature quenching rate coefficient of argon is more than two orders of magnitude smaller than the one for water.[15] From lifetime measurements in the flow reactor, the spontaneous emission rate was found to be $2.8 \cdot 10^7$ s$^{-1}$ in agreement with Ref. 17, and the measured quenching rate in the flame was rate $6 \cdot 10^7$ s$^{-1}$ at 40 mm height above the burner. If it is assumed that the total quenching is caused by water, it can be concluded from the $H_2O$ concentration that the quenching rate coefficient for $O(3p^3P)$ by water is about $1.3 \cdot 10^{-9}$ cm$^3$/s at 1350 K, which is almost a factor of 3 lower than the value of $4.9 \cdot 10^{-9}$ cm$^3$/s measured at room temperature.[15] If the contribution of Ar would be larger, the rate coefficient for water would become even smaller. Such a decrease of the quenching rate coefficient with increasing temperature would be expected when the collision proceeds via an attractive potential surface. This assumption is also supported by the large room temperature value.

### Calculation of the Calibration Factors $C_Q$:

To calculate the quenching calibration factor $C_Q$ in Eq. (3), we solved the system of coupled differential equations (1a,b,c) for different values of $Q_2$. Additional input parameters required were the two-photon absorption cross section $\alpha_{12}$, the photoionization cross section $\sigma_{2i}$, and the spontaneous transition probabilities $A_{31}$ and $A_{23}$. Values for $\sigma_{2i}$ and $\alpha_{12}$ have been reported recently;[13,18] $A_{31}$ was taken from Ref. 17, and for $A_{23}$ we used our measured value of $2.8 \cdot 10^7$ s$^{-1}$. For the laser power density $I_L$ we used an analytical expression of the form $I_L = a \cdot t^b \cdot \exp(-ct)$, where the parameters $a$, $b$, and $c$ where chosen so that the resulting simulated pulse resembled a measured one with respect to peak intensity, pulse energy and half width. Calculations showed that the temporal shape of the pulse has only little effect on $C_Q$. In a multimode laser system, mode-beating can lead to short-time high intensity peaks which can not be detected with our available time resolution. However, if a large number of modes occur during a pulse, these peaks will be less pronounced, and in addition, their effect will be "damped" somewhat by the calibration procedure.

The calculations were performed assuming a flat spatial laser beam profile. The actual profile is very similar to a Gaussian, which does not change the value of $C_Q$ significantly compared to a flat profile, for the same reason that applies to the dependence on peak intensity (see Table II).

The calculation yields an almost linear dependence of $C_Q$ on $Q_2$ with a slope of $3.08 \cdot 10^{-9}$ s for a peak power density of $1.1 \cdot 10^8$ W/cm$^2$. This linear relationship holds as long as the quenching rate

in the flame is much larger than in the flow reactor and the pumping rate $W_{12}$ is small compared to the spontaneous emission rate $A_{23}$; both conditions are fulfilled in our case. If the quenching rates in the flame and in the reactor are equal, $C_Q$ becomes unity. For the flames investigated, the values of $C_Q$ are between 1.2 and 1.5.

### Sensitivity of $C_Q$ to Atomic and Experimental Parameters:

As can be seen from Eq. (3), the atom concentration in the flame is proportional to the calibration factor $C_Q$; therefore, the accuracy of the derived atom concentrations depends on the reliability of this factor, which is, in turn, dependent on saturation, photoionization and laser photolysis conditions. In this section, we shall discuss the influence of these parameters on $C_Q$.

### Saturation:

For this section, we shall first assume that fluorescence signals are not affected by ionization of the excited state or production of additional atoms by photodissociation. For high laser intensities the ground state will be noticeably depopulated. The onset of saturation occurs at lower intensities in the flow reactor than in the flame, since the faster quenching under flame conditions helps to repopulate the ground state, inhibiting saturation. This is illustrated in Fig. 3a. Populations of level 2 are plotted on a double logarithmic scale as a function of laser intensity for quenching rates of zero (upper curve) and $1.5 \cdot 10^8$ s$^{-1}$. The calculations were performed with a value for $\alpha_{12}$ of $5.5 \cdot 10^{-28}$ cm$^4$/W as reported in Ref. 13. For low intensities, both curves have a slope of 2, corresponding to a two-photon transition. At intensities higher than those typically used in our experiments, the upper curve has a slope lower than 2. This implies that the value of $C_Q$, which is equal to the ratio of the populations with and without quenching at a given intensity, becomes smaller. A higher value for $\alpha_{12}$ has qualitatively the same effect; however, while the pumping rate is linear with respect to $\alpha_{12}$, is quadratically dependent on $I_L$.

### Ionization:

If the excited state is depopulated by ionization after absorption of a third photon, the effect described above becomes enhanced. Fig. 3b shows the same calculation as in Fig. 3a except that now ionization of level 2 is included; for the cross section, the value of $\sigma_{2i} = 5.3 \cdot 10^{-19}$ cm$^2$ from ref. 13 was used. The deviation from a quadratic power dependence becomes more pronounced than in Fig. 3a. The lower curve levels out less rapidly since

quenching competes with ionization, decreasing the ionization rate. Actually power dependences with exponents between 1.65 and 1.95 have been measured in our experiments for power densities between about 0.6 and $6.0 \cdot 10^8$ W/cm$^2$, the lower values resulting from measurements in the discharge flow reactor. From this result it can be concluded that the input parameters are at least of the right order of magnitude, although it should be noted that power dependences are not too sensitive to e.g. $\sigma_{2i}$ over the experimentally accessible intensity range, so that measuring power dependences is no suitable way to determine ionization cross sections.

Table II summarizes the results of the described model calculations. Calibration factors $C_Q$ resulting from a quenching rate of $1.5 \cdot 10^8$ s$^{-1}$ are given for different laser intensities, ionization cross sections and two-photon absorption cross section. Also quoted are the deviations from a standard value of $C_Q$, which was calculated with the values of $\alpha_{12}$ and $\sigma_{2i}$
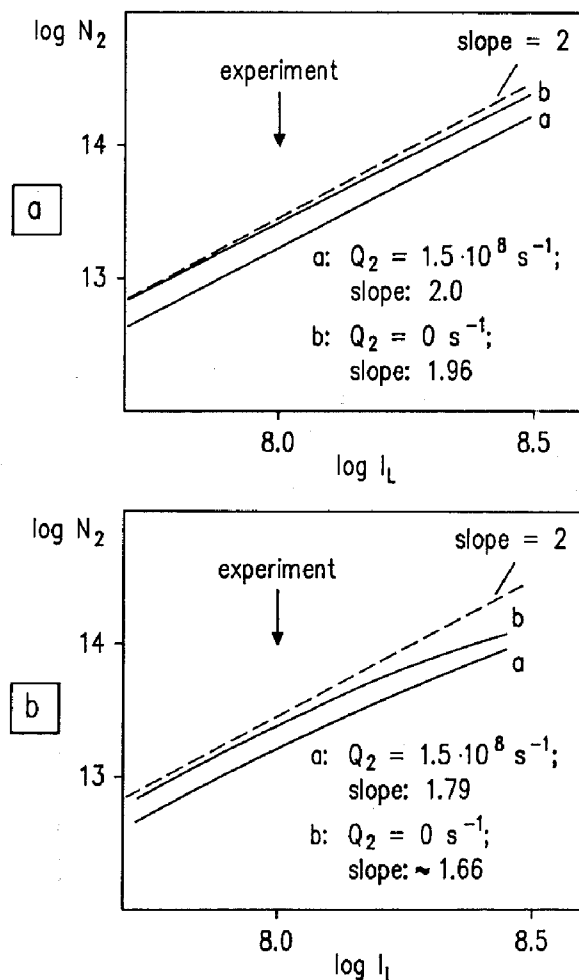


FIG. 3. Effect of saturation (a) and saturation combined with photoionization (b) on the dependence of two-photon excited fluorescence signals on laser intensity; arrows indicate highest laser intensity used in the experiments

## TABLE II

Sensitivity of the calibration factor $C_O$ to laser intensity $I_L$, ionization- and two-photon absorption cross sections; standard values (centre of table): $I_{L,0} = 1.1 \cdot 10^8$ W/cm$^2$; $\alpha_{12,0} = 5.5 \cdot 10^{-28}$ cm$^4$/W, $\sigma_{2i,0} = 5.3 \cdot 10^{-19}$ cm$^2$; deviation (in %) from standard set in brackets; quenching rate: $1.5 \cdot 10^8$ s$^{-1}$

| $\sigma_{2i}$ | $I_L$: | $0.2 \cdot I_{L,0}$ | | | $1.0 \cdot I_{L,0}$ | | | $5.0 \cdot I_{L,0}$ | | |
|---|---|---|---|---|---|---|---|---|---|---|
| | $\alpha_{12}$: | $\alpha_{12,0}\cdot 0.2$ | $\alpha_{12,0}\cdot 1.0$ | $\alpha_{12,0}\cdot 5.0$ | $\alpha_{12,0}\cdot 0.2$ | $\alpha_{12,0}\cdot 1.0$ | $\alpha_{12,0}\cdot 5.0$ | $\alpha_{12,0}\cdot 0.2$ | $\alpha_{12,0}\cdot 1.0$ | $\alpha_{12,0}\cdot 5.0$ |
| $\sigma_{2i,0}\cdot 0.2$ | | 1.60 (7.1) | 1.60 (7.1) | 1.59 (6.5) | 1.57 (5.2) | 1.56 (5.0) | 1.53 (2.6) | 1.46 (2.0) | 1.34 (10.6) | 1.12 (28.2) |
| $\sigma_{2i,0}\cdot 1.0$ | | 1.57 (5.2) | 1.57 (5.2) | 1.57 (5.2) | 1.49 (0.0) | 1.49 (—) | 1.46 (2.0) | 1.25 (10.8) | 1.18 (23.2) | 1.08 (31.9) |
| $\sigma_{2i,0}\cdot 5.0$ | | 1.49 (0.0) | 1.49 (0.0) | 1.49 (0.0) | 1.28 (15.2) | 1.28 (15.2) | 1.25 (17.5) | 1.08 (31.9) | 1.06 (33.7) | 1.05 (34.6) |

given in Ref. 14 and a laser intensity of $1.1 \cdot 10^8$ W/cm$^2$, the highest intensity for which no noticeable saturation was found. Therefore, $C_O$ responds less sensitively to a decrease of $\alpha_{12}$, $\sigma_{2i}$ or $I_L$ than to an increase of these quantities. The data in Table II underline the basic idea of the calibration method, that is, to obtain quantitative atom concentrations from a fluorescence experiment which are only weakly sensitive to atomic and experimental parameters.

### Photodissociation:

It has been shown that in $H_2/O_2/Ar$ flames at atmospheric pressure, O atom production by dissociation of vibrationally excited $O_2$ can contribute significantly to the atom concentration detected by two-photon excited fluorescence.[6] There is evidence that also the measurements in the low-pressure flames investigated here are affected by photodissociation, if high laser intensities are applied.

If additional atoms are produced photolytically, the fluorescence signal shows a $I_L^n$ dependence on laser intensity with an exponent $n$ larger than without photolysis. For high laser intensities, measurements of the dependence of fluorescence intensity on laser power density in our flames yielded exponents larger than expected for a system that is not affected by photodissociation. The measured exponents ranged between 1.89 and 2.15 with standard deviations of usually $\pm 6\%$ for laser power densities between $2 \cdot 10^7$ and $2 \cdot 10^8$ W/cm$^2$ whereas calculations showed that without photolysis, an exponent of about 1.8 had to be expected.

This effect may in principle be used to calculate the fraction of photolytically produced O atoms. Practically, however, this procedure is not very accurate since small changes of the power exponent are associated with large changes in the relative amount of O atoms produced by laser photolysis: calculations showed that a difference of 10% in the exponent results in a change of 40% in the atom concentrations. More reliable results can be obtained by successive measurements of O atom concentrations with stepwise reduction of the laser power density. Since the amount of photolytically produced atoms depends linearly on the laser power density, it can be concluded that the measurements are not affected by photodissociation as long as the observed O atom concentrations exhibit no dependence on laser intensity.

Figure 4 shows measured concentration profiles of oxygen atoms in three $H_2/O_2/Ar$ flames with different equivalence ratios, together with the results of model calculations. The error bars represent the overall uncertainty, resulting from a statistical error of 15% and an additional estimated error in $C_0$ of 10% (see Table II). All three profiles were measured with laser power densities around $5 \cdot 10^6$ W/cm$^2$. In this range, the measured O atom concentrations showed no dependence on laser intensity, so that photolytic production could not contribute significantly to the measured atom concentrations; this result was also supported by model calculations. The agreement between measurements and model calculations is good for the lean and stoichiometric flames. The disagreement in the case of the rich flame is probably due to larger uncertainties in the measured temperature profile for this flame.

### Summary

The application of two-photon laser-induced fluorescence for the measurement of absolute O atom number densities in low pressure flames has been discussed. The loss of fluorescence signal under flame conditions due to quenching is accounted for by measuring quenching is accounted for by measuring quenching rates from time decays of the fluorescence signals and calculating the relative populations in the excited state under different quenching conditions. The influence of saturation due to the
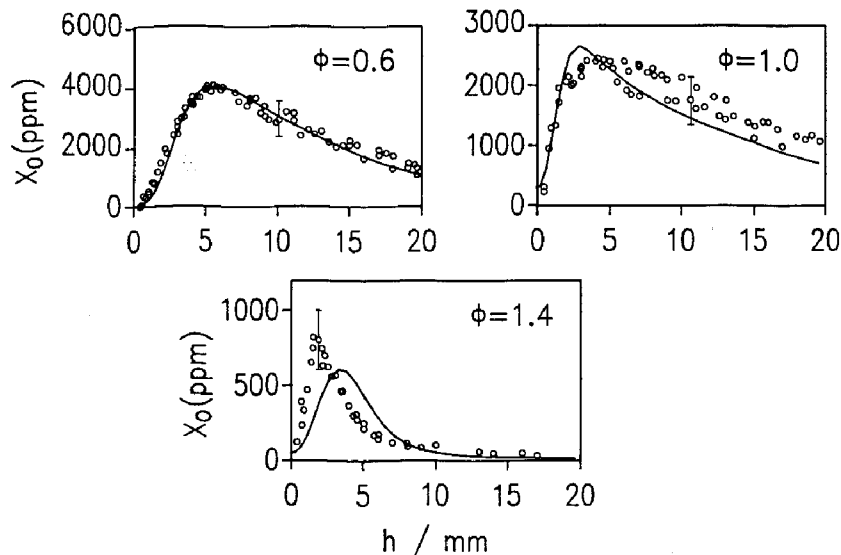
FIG. 4. O atom concentrations in $H_2/O_2/Ar$ flames, $p = 95$ mbar (72 Torr); a: flame 1, equivalence ratio 0.6, temperature 1350 K; b: flame 2, equivalence ratio 1.0, temperature 1350 K; c: flame 3, equivalence ratio 1.4, temperature 1100 K (———): model; the error bar indicates overall uncertainty

high power densities necessary for a two-photon process, of photoionization and photodissociation is discussed. It is shown that the calibration technique using a flow reactor makes concentration measurements relatively insensitive to uncertainties in experimental parameters like laser power density, or atomic quantities like two-photon absorption or ionization cross sections. However, for the highest power densities applied in our experiments, photolytic production of O atoms may become a problem. Since it is difficult to correct measured number densities with respect to photodissociation subsequently, it is necessary to use high detection sensitivity for the fluorescence radiation in order to perform experiments at sufficiently low power densities.

Basically, application of the technique described in this paper to hydrocarbon flames as well as to flames at atmospheric pressure is desirable. However, in these flames the problem of photodissociation may become more severe, as can be seen from the results in ref. 10 and a preliminary investigation of a fuel-rich atmospheric pressure methane/air flame performed in our group. Both the measured fluorescence intensity profile in the flame and the dependence of fluorescence on laser intensity showed that, at least in the burnt-gas region, virtually all O atoms were produced photolytically. These measurements were performed with a comparatively high laser intensity of $>10^8$ W/cm$^2$. However, experiments with reduced laser intensity turned out to be difficult, since at least in fuel-rich hydrocarbon flames, a strong background emission of the flame around 845 nm was observed, which leads to insufficient signal-to-noise ratios at lower

laser intensities. Therefore, a successful application of the method described here to atmospheric pressure hydrocarbon flames without major changes in the detection and/or excitation system are questionable.

## REFERENCES

1. KOHSE-HÖINGHAUS, K., KOCZAR, P. AND JUST, TH.: Twenty First Symposium (International) on Combustion; p 1719 The Combustion Institute, (1988).
2. KOHSE-HÖINGHAUS, K., KELM, S., MEIER, U., BITTNER, J. AND JUST, TH.: Complex Chemical Reaction Systems. Mathematical Modelling and Simulation; (J. Warnatz, W. Jäger Eds.); Springer, Heidelberg 1987.
3. BITTNER, J., KOHSE-HÖINGHAUS, K., MEIER, U., KELM, S. AND JUST, TH.: Comb. Flame 71, 41 (1988).
4. DASCH, C. J. AND BECHTEL, J. H.: Opt. Lett. 6, 36 (1981).
5. TEETS, R. E. AND BECHTEL, J. H.: Opt. Lett. 6, 458 (1981).
6. GOLDSMITH, J. E. M.: Appl. Opt. 26, 3566 (1987).

7. Miziolek, A. W. and DeWilde, M. A.: Opt. Lett. 9, 390 (1984).

8. Alden, M. A., Hertz, H. M., Svanberg, S. and Wallin, S.: Appl. Opt. 23, 3255 (1984).

9. Goldsmith, J. E. M.: J. Chem. Phys. 78, 1610 (1983).

10. Goldsmith, J. E. M.: Twentieth Symposium (International) on Combustion; p 1331, The Combustion Institute 1985.

11. Goldsmith, J. E. M.: Opt. Lett. 11, 416 (1986).

12. Meier, U., Kohse-Höinghaus, K. and Just, Th.: Chem. Phys. Lett. 126, 567 (1986).

13. Bamford, D. J., Jusinski, L. E. and Bischel, W. K.: Phys Rev. A34, 185 (1986).

14. Bischel, W. K., Perry, B. E. and Crosley, D. R.: Appl. Opt. 21, 1419 (1982).

15. Bittner, J., Kohse-Höinghaus, K., Meier, U. and Just, Th.: Chem. Phys. Lett. 143, 571 (1988).

16. Warnatz, J.: Ber. Bunsenges. Phys. Chem. 82, 834 (1978).

17. Wiese, W. L., Smith, M. W. and Glennon, B. M.: Atomic Transition Probabilities Vol. 1: Hydrogen through Neon; National Standard Reference Data Series, National Bureau of Standards 4, Washington D.C. 1966.

18. Saxon, R. P. and Eichler, J.: Phys. Rev. A34, 199 (1986).

# COMMENTS

*J. E. M. Goldsmith, Sandia National Laboratories, USA.* From your measurement in the atmospheric-pressure hydrocarbon flame, it appears that photochemical creation of atomic oxygen in flames is a more severe problem at atmospheric pressure than it is at reduced pressure. I have seen similar effects in hydrogen flames. Do you believe that this difference is due solely to the decrease in radical concentrations relative to stable species concentrations at the higher pressure, or do other factors play a role as well?

### REFERENCE

1. J. E. M. Goldsmith, "Applied Optics 26, 3566 (1987).

*Author's Reply.* If we compare O atom measurements with equally high laser intensities in the burnt gas of fuel-rich 1) $H_2/O_2/Ar$ flames at low pressure, 2) $CH_4/O_2$ flames at low pressure and 3) $CH_4/O_2$ flames at atmospheric pressure, it is interesting to note that the relative amount of O atoms produced photolytically is comparable in the two methane flames which have approximately the same chemical composition and temperature, whereas for the diluted hydrogen flame with significantly lower temperature, the extent of photolytical O atom production is lower. This leads to the conclusion that besides the ratio between radicals and stable species, also temperature (via T-dependent dissociation cross sections) and chemical composition (via more potential O atom precursors in hydrocarbon than in hydrogen flames) may play a role.

•

*R. P. Lucht, Sandia National Laboratories, USA.*

What species gives rise to the emission interference in atmospheric pressure flames?

*Author's Reply.* We have not yet identified the source of the background emission, which is observed also in low-pressure flames. However, it has to be a hydrocarbon species since the emission does not occur in $H_2/O_2/Ar$ flames, but in both $CH_4/O_2$ and $C_2H_2/O_2$ flames, and here mainly under fuel-rich conditions.

•

*N. M. Laurendeau, Purdue Univ., USA.* How much shift do you see in the O-atom profile if no correction for quenching is made? Also please comment on the reasons for the greater disagreement between the calculated and experimental oxygen atom profiles.

*Author's Reply.* The shift in the position of the peak O atom concentration depends to some extent on the flame under investigation; however, it was usually 1 mm or less.

The $\Phi = 1.4$ $H_2/O_2/Ar$ flame is the only flame where the disagreement exceeds the experimental error bars. In this case, probably an uncertainty in the temperature profile leads to the difference between model and experiment, since the O atom peak concentration occurs at low heights above the burner where the temperature has a comparatively large gradient. The stated experiment error bars do not include uncertainties in the temperature profile.

•

*J. B. Jeffries, SRI International, USA.* Could you comment on the choice between detection of the fluorescence in the directly excited triplet system

at 845 nm or detection of the fluorescence from the energy transfer into the quintet system at 775 nm.

*Author's Reply.* Although the sensitivity of our detection system is higher at 777 than at 845 nm, we cannot exploit it since in the case of the ref-

erence measurement in the discharge flow reactor, the energy transfer to the quintet system is too inefficient to produce a sufficiently high population in the SP state; this is due to the considerably lower pressure.